Article

Noradrenaline Specific, Efficient Visualization in Brain Tissue Triggered by Unique 'Cascade' Nucleophilic Substitution

Yongkang Yue, Fangjun Huo, and Caixia Yin

Anal. Chem., **Just Accepted Manuscript** • DOI: 10.1021/acs.analchem.8b04836 • Publication Date (Web): 28 Dec 2018

Noradrenaline Specific, Efficient Visualization in Brain Tissue Triggered by Unique 'Cascade' Nucleophilic Substitution

Yongkang Yue,[†] Fangjun Huo,[‡] Caixia Yin[†,*]

[†]Key Laboratory of Chemical Biology and Molecular Engineering of Ministry of Education, Key Laboratory of Materials for Energy Conversion and Storage of Shanxi Province, Institute of Molecular Science, Shanxi University. Taiyuan 030006, China. E-mail: yincx@sxu.edu.cn. Tel/Fax: +86-351-7011022.

[‡]Research Institute of Applied Chemistry, Shanxi University, Taiyuan 030006, China.

ABSTRACT: Noradrenaline as one of the most important neurotransmitters in sympathetic nervous system plays key roles in all of the forebrain activities such as perception, memory, learning, and homeostasis and its dysfunction is closely related to both neurodegenerative diseases and central nervous system disorders. The very similar structures and properties of the three co-existed catecholamine neurotransmitters: dopamine, epinephrine, noradrenaline make it almost impossible to design fluorescent probes that respond specifically to noradrenaline which astricted its physiological and pathological studies greatly. Fantastic design turned dreams into reality in this work: the cascade nucleophilic substitution reactions between noradrenaline and fluorophore coupling carbonic ester which formed a five-membered ring catechol-containing compound with the release of the fluorophore accompanied by unique fluorescent responses allow us to develop fluorescent probe to detect and visualize noradrenaline over dopamine and epinephrine in brain tissue. Instead of the noradrenaline synzyme immunofluorescence labeling path, the present fluorescent probe can visualize noradrenaline directly with comparable specificity.

Perception, memory, learning, and homeostasis are mediated by the release and accumulation of neurotransmitters in our brain.[1] Typically, catecholamine derivates such as dopamine, noradrenaline (norepinephrine), and epinephrine are principal neurotransmitters in the sympathetic nervous system. In neurons, the three siblings are synthesized from tyrosine via a series of enzymatic reaction and stored in the acidic synaptic vesicles (pH 5.0-5.5) with high concentration (~mM, Figure 1).[2-4] As one of the most important neurotransmitters, noradrenaline plays key roles in all of the forebrain activities and its dysfunction is closely related to both neurodegenerative diseases and central nervous system disorders.[5-7] Besides, noradrenaline has been used as first-line vasopressor agents in the treatment of shock.[8,9] Promoted by its vital functions and increasing incidence of noradrenaline related diseases, the physiological and pathological studies attracted more and more attention in recent years.[10-14]

In 2009, Sames and coworkers designed fluorescent false neurotransmitters to visualize the release of dopamine in the striatum under stimulation and made excellent progresses based on this strategy.[15-18] Recently, they developed the FFN270 as fluorescent false neurotransmitter to noradrenergic synapses in brain tissue specifically.[19] These substrates can image the neurotransmitters release and the activity of synapses in living tissue. However, the *in situ* noradrenaline analysis which is extremely important for its biological roles is restricted. Fluorescent probes with specific responses toward noradrenaline are supra tools for its further study.[14,19] Representatively, the Glass group utilized coumarin aldehyde derivates (NeuroSensor 521 and NeuroSensor 715) as fluorescent probes for monoamines neurotransmitters detection via the formation of Schiff base.[20,21] For the probes based on this design strategy, they can also react with generic amines such as glutamate featuring even more pronounced fluorescence responses compared with their reaction with catecholamines because of the quenching nature of the catechol group in catecholamine neurotransmitters through photo-induced electron transfer process.[22-24] Besides, the discrimination of dopamine and noradrenaline cannot be realized by this strategy, which may block its application in tissue specific noradrenaline imaging. In 2014, the Kleinfeld group modified the G-protein with α_{1A} adrenergic receptor to detect noradrenaline release indirectly via the activation of receptor triggered cytosolic Ca^{2+} increase which was detected by a genetically encoded FRET based Ca^{2+} sensor.[14] For this strategy based Ca^{2+} probes, the cellular sliced neurotransmitters cannot be directly detected. Thus, new strategy for noradrenaline specific fluorescent probes design is imperative to elucidating the effect of noradrenaline in brain.

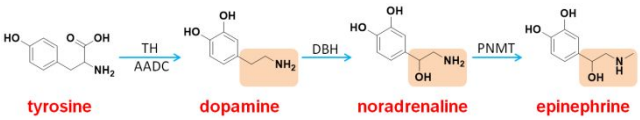

Figure 1. Catecholamine neurotransmitters and their biosynthesis. Tyrosine hydroxylase (TH), aromatic amino acid decarboxylase (AADC), dopamine-β-hydroxylase (DBH), phenylethanolamine N-methyltransferase (PNMT).

For the three siblings, the inherent 2-aminoethanol moiety of noradrenaline may react with fluorophore coupling carbonic ester via cascade nucleophilic substitution reactions to form a five-membered ring compound with the release of the fluorophore (Figure 2). The reaction process can promote the

specificity of fluorescent probes toward noradrenaline over other generic amines, dopamine, and epinephrine. Besides, the cleavage detection mechanism can effectively avoid the fluorescent quench caused by the aforementioned intramolecular PET process. Holding this in mind, we firstly synthesized a coumarin based carbonic ester derivate **CNE**. **CNE** featured strong fluorescent emission at 394 nm which was induced by the weak electron-withdrawing effect of carbonic ester moiety and non-fluorescent response displayed upon the addition of noradrenaline (Figure S1). To effectively modulate the fluorescence of the probe during the detection process, we forecasted that fluorescein derivates with spiro ring-closing and -opening process might be suitable candidates for probes construction. Indeed, the introduction of ethyl carbonate to fluorescein quenched its fluorescent emission (**FHE**, Figure S2). But noradrenaline addition did not cause significant fluorescent change of **FHE** containing detection system within one hour. To activate the reaction site, we further combined 4-methylthiophenol with fluorescein through carbonyl to synthesize probes **FHS** and **FCS** for noradrenaline detection. The thiophenol moiety as the primary leaving group could facilely be replaced by amino which initiated the detection process. [25-27] Exhilaratingly, both **FHS** and **FCS** could react with noradrenaline exhibited turn-on fluorescent responses. Featuring better water solubility, **FCS** was used for further spectroscopic evaluation and brain tissue noradrenaline imaging.

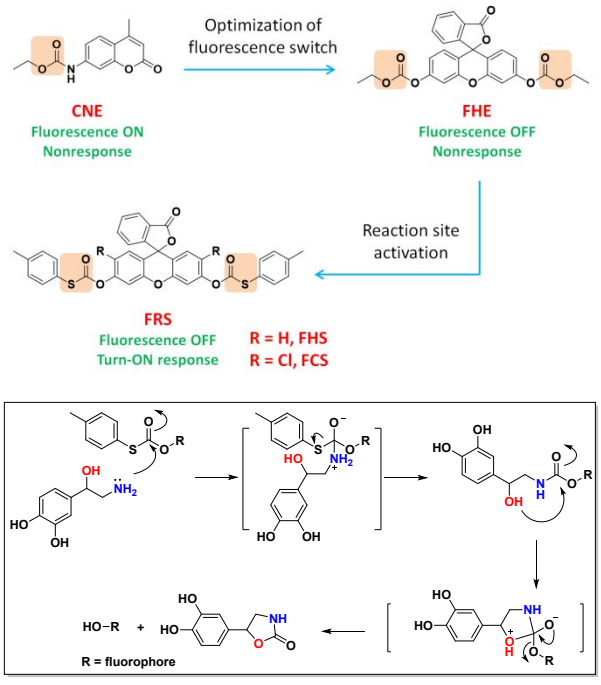

Figure 2. Fluorescent probes design and the detection mechanism of **FRS** toward noradrenaline.

EXPERIMENTAL SECTION

Materials and Methods. All chemicals were purchased from commercial suppliers and used without further purification. All solvents were purified prior to use. Distilled water was used after passing through a water ultra-purification system. TLC analysis was performed using precoated silica plates. Hitachi F−7000 fluorescence spectrophotometer was employed to measure fluorescence spectra. Hitachi U-3900 UV-vis spectrophotometer was employed to measure UV-vis spectra. Shanhai Huamei Experiment Instrument Plants, China provided a PO-120 quartz cuvette (10 mm). ^{1}H NMR and ^{13}C NMR experiments were performed with a BRUKER AVANCE III HD 600 MHz and 151 MHz NMR spectrometer, respectively (Bruker, Billerica, MA). Coupling constants (*J* values) are reported in hertz. HR-MS determinations were carried out on an Thermo Scientific Q Exactive Instruments. The brain tissue imaging experiments were measured by Olympus Fluo View FV1000 laser-scanning microscope with an objective lens (×20).

Synthesis. Compounds were synthesized according to the procedure in Scheme S1-S3 in the Supporting Information.

*Synthesis of **CNE**.* *m*-Aminophenol (5 mmol) was dissolved in ethyl acetate and the solution was refluxed for 30 min. Then, ethyl chloroformate (0.5 equiv.) was added dropwise. The solution was cooled to room temperature after white solid precipitated. After filtration and washing with ethyl acetate, compound **1** was obtained as white solid and used for further synthesis directly.

In the compound **1** (1 mmol) and ethyl acetoacetate (2 equiv.) system, concentrated sulfuric acid (2 drops) was added. The mixture was stirred for 10 h under room temperature. After that, H_2O was added and the mixture was filtrated to obtain probe **CNE** as white solid. ^{1}H NMR (600 MHz, DMSO-d_6) δ 10.14 (s, 1H), 7.69 (d, J = 8.6 Hz, 1H), 7.55 (s, 1H), 7.41 (d, J = 8.6 Hz, 1H), 6.23 (s, 1H), 4.17 (q, J = 7.0 Hz, 2H), 2.39 (s, 3H), 1.27 (t, J = 7.0 Hz, 3H). ^{13}C NMR (151 MHz, DMSO-d_6) δ 160.5, 154.3, 153.8, 153.7, 143.3, 126.5, 114.7, 114.7, 112.3, 104.8, 61.2, 18.5, 14.9.

*Synthesis of **FHE**.* In a fluorescein (1 mmol) contained THF (10 mL) system, Et_3N (2 equiv.) was added. Then, ethyl chloroformate (3 equiv.) was added dropwise under ice bath. The mixture was stirred for 10 h under room temperature before filtration. The obtained filtrate was concentrated under reduced pressure and purified by column chromatography using ethyl acetate / petroleum ether (1 / 6) as eluent to give **FHE** as a white solid. ^{1}H NMR (600 MHz, DMSO-d_6) δ 8.07 (d, J = 7.6 Hz, 1H), 7.83 (t, J = 7.3 Hz, 1H), 7.77 (t, J = 7.4 Hz, 1H), 7.42 (d, J = 8.2 Hz, 3H), 7.06 (d, J = 8.7 Hz, 2H), 6.92 (d, J = 8.7 Hz, 2H), 4.28 (q, J = 7.0 Hz, 4H), 1.30 (t, J = 7.1 Hz, 6H). ^{13}C NMR (151 MHz, DMSO-d_6) δ 168.8, 152.8, 152.6, 152.6, 151.2, 136.5, 131.1, 129.8, 125.8, 125.5, 124.6, 118.5, 116.9, 110.5, 81.3, 65.5, 14.4.

*Synthesis of **FRS**.* To a solution of *p*-toluenethiol (10 mmol) and triphosgene (0.5 equiv.) in CH_2Cl_2 (20 mL) at 0 °C, pyridine (1 equiv. in 5 mL CH_2Cl_2) was added dropwise. The mixture was stirred for 1 h at 0 °C and then poured into 100 mL H_2O. The organic layer was separated, washed with H_2O, dried with sodiumfulfate, and concentrated under reduced pressure. The obtained crude product of compound **2** was used for further synthesis directly.

Fluorescein or 2',7'-dichlorofluorescein (1 mmol) and Et_3N (2 equiv.) was dissolved in 20 mL CH_2Cl_2. Compound **2** (2 equiv. in 5 mL CH_2Cl_2) was then added at 0 °C. The mixture was gradually warmed to room temperature and continued to react for 10 h. After that, the solvent was removed under reduced pressure and the residue was separated by column chromatography using ethyl acetate / petroleum ether (1 / 6) as eluent to give **FRS** as a white solid.

FHS: ^{1}H NMR (600 MHz, DMSO-d_6) δ 8.06 (d, J = 7.6 Hz, 1H), 7.80 (t, J = 7.1 Hz, 1H), 7.75 (t, J = 7.4 Hz, 1H), 7.53 (d, J = 8.1 Hz, 4H), 7.44 (d, J = 2.3 Hz, 2H), 7.37 (d, J = 7.6 Hz, 1H), 7.30 (d, J = 8.0 Hz, 4H), 7.07 (dd, J = 8.7, 2.3 Hz, 2H), 6.92 (d, J = 8.7 Hz, 2H), 2.33 (s, 6H). ^{13}C NMR (151 MHz, DMSO-d_6) δ 168.8, 168.4, 152.5, 152.5, 151.2, 140.8, 136.5, 135.2, 131.1, 130.7, 129.9, 125.8, 125.6, 124.6, 123.1, 118.6, 117.3, 110.7, 81.1, 21.3.

FCS: ^{1}H NMR (600 MHz, DMSO-d_6) δ 8.05 (d, J = 7.6 Hz, 1H), 7.86 – 7.74 (m, 4H), 7.54 (d, J = 8.1 Hz, 4H), 7.46 (d, J = 7.6 Hz, 1H), 7.32 (d, J = 8.1 Hz, 4H), 7.12 (s, 2H), 2.35 (s, 6H). ^{13}C NMR (151 MHz, DMSO-d_6) δ 168.4, 167.9, 151.7, 149.7, 148.6, 141.0, 136.6, 135.6, 135.2, 131.4, 130.8, 129.4, 126.1, 125.8, 124.5, 122.6, 122.1, 118.9, 113.8, 79.9, 21.3. HR MS $[M+H]^+$: m/z Calcd 701.0257, Found 701.0259.

Preparation of Stock Solutions of Probes and Analytes. Stock solutions of probe **CNE**, **FHE**, **FHS**, and **FCS** (2 mM) were prepared in DMSO. Stock solutions of 100 mM dopamine, epinephrine, noradrenaline, and glutamate were prepared by dissolution in PB (pH 5.0, 50 mM $Na_2S_2O_3$, 120 mM NaCl) separately. Stock solutions of 100 mM GSH and Gly were prepared by dissolution in PB (pH 5.0). All chemicals used were of analytical grade.

General Fluorescence Spectra Measurements. All the detection experiments were measured in PB−DMSO (pH 5.0, 1 / 1, v / v). The procedure was as follows: into a PB−DMSO (pH 5.0, 1 / 1, v / v) solution, containing 5 μM **FCS**, an analyte sample was added. The process was monitored by fluorescence spectrometer (λ_{ex} = 510 nm, slit: 5 nm / 2.5 nm).

Brain Tissue Preparation. All animal protocols were approved by the Department of Science & Technology of Shandong Province. The SD mice (6- to 7-week-old, female) were obtained from Yantai Raphael Biotechnology SPF barrier environment animal house and acclimatized to the animal facility for at least 5 days. After quarantine, qualified animals were maintained under 12 h light / dark cycles at room temperature 23 ± 3 °C with 40−70 % humidity. Mice were anesthetized with thiobutabarbital (100 mg/kg intraperitoneal injection) and intracardially perfused with PBS, 4 % paraformaldehyde sequentially. The brains were collected and fixed for 1-2 hours and then cryopreserved in 30 % sucrose at 4 °C. Then, the coronal 40 μm sections were collected and stored in a cryoprotectant at -20 °C for immunohistochemical treatment.

Immunohistofluorescence. The sections were processed either for TH and DBH dual labeling, or DBH and PNMT dual labeling which were then stained with **FCS** before imaging, respectively. For TH and DBH dual labeling experiments, the sections were processed with a primary antibody cocktail of Rabbit Anti-Tyrosine Hydroxylase Polyclonal Antibody (1:500, bs-0016R; Bioss Antibodies) and Anti-Dopamine β Hydroxylase (1:1000, MAB308; Millipore) for 2 h followed by a secondary antibody cocktail of Goat Anti-Rabbit IgG / Cy3 (1:250, bs-0295G-Cy3; Bioss Antibodies) and Goat Anti-Mouse IgG / ALexa Fluor 350 (1:100, bs-0296G-AF350; Bioss Antibodies) for 30 min, which were then stained with **FCS** (5 μM) for 30 min. For PNMT and DBH dual labeling experiments, the sections were processed with a primary antibody cocktail of Rabbit Anti-PNMT Polyclonal Antibody (1:500, bs-3912R; Bioss Antibodies) and Anti-Dopamine β Hydroxylase (1:1000, MAB308; Millipore) for 2 h followed by a secondary antibody cocktail of Goat Anti-Rabbit IgG / Cy3 (1:250, bs-0295G-Cy3; Bioss Antibodies) and Goat Anti-Mouse IgG / ALexa Fluor 350 (1:100, bs-0296G-AF350; Bioss Antibodies) for 30 min, which were then stained with **FCS** (5 μM) for 30 min. All these experiments were processed at 37 °C.

RESULTS AND DISCUSSION

Detection Properties of FCS Toward Noradrenaline in Solution. The aforementioned fluorescent detection mechanism of **FCS** toward noradrenaline was firstly validated upon HR-MS characterization of the reaction mixture. As shown in Figure S18 (detailed in Scheme S4), the signals of both the intermediate products (compound **3** and **4**) and the ultimate products (compound **5** and 2',7'-dichlorofluorescein) were occurred distinctly. Besides, the UV-vis absorption spectra comparison of the **FCS**-noradrenaline system and 2',7'-dichlorofluorescein demonstrated the production of 2',7'-dichlorofluorescein in the detection process (Figure S13). The results sustained our design assumption.

The detection property of **FCS** toward noradrenaline was then valued systematically. **FCS** itself displayed non-fluorescent emission in the detection system. Upon noradrenaline addition, distinct fluorescent emission at 530 nm enhanced gradually (Figure 3a). Correspondingly, in the UV-vis spectra, a new absorption peak at 511 nm enhanced (Figure 3b). As for noradrenaline probes, the most challenging parameter was the specificity over dopamine and epinephrine. Thus, we added equal amount of dopamine or epinephrine to **FCS** containing system under the same condition with noradrenaline detection. As we designed, both dopamine and epinephrine induced one-eighth fluorescent intensities enhancement compared with noradrenaline (Figure 3c and Figure S3, S4). Besides, the responses of **FCS** toward 5 mM other generic amines such as glutamate, glycine, the major reducing substance GSH, and 500 μM lysine, 2-aminoethanol containing amino acid such as threonine and serine were valued and none of them induced distinct fluorescent change of **FCS** in the detection system (Figure S5-S10). [20,21,28] Cys with similar mercaptoethylamine moiety was also evaluated and 50 μM cysteine did not induce significant fluorescent response (the cellular concentration of unbounded cysteine is nM~μM, Figure S11).[29,30] Because of the readily oxidized nature of noradrenaline, we set 320 min as the reaction period in the quantitative studies to minimize the oxidation induced noradrenaline consumption. The fluorescent intensities of the reaction system at 530 nm were linear with the concentrations of noradrenaline (0-1 mM, Figure 3d and Figure S12). These results demonstrated that **FCS** could be used for noradrenaline specific detection *in vitro*.

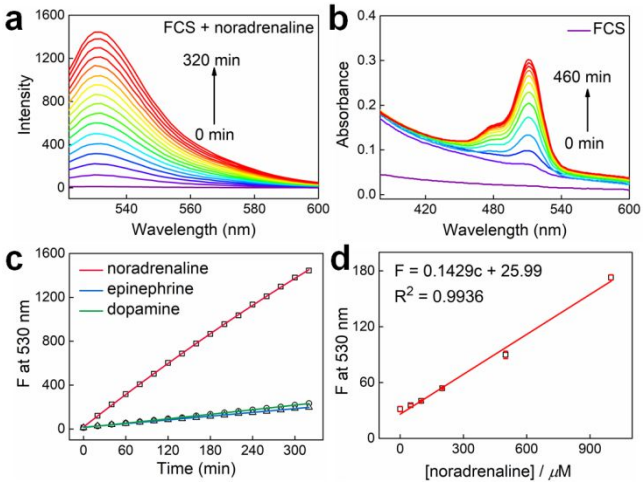

Figure 3. Spectroscopic responses of **FCS** toward noradrenaline, dopamine, and epinephrine. Time-dependent fluorescent (a) and UV-vis (b) responses of 5 μM **FCS** toward 5 mM noradrenaline in PB−DMSO (pH 5.0, 1:1, v/v) system. (c) Time-dependent fluorescent intensities changes of 5 μM **FCS** toward 5 mM noradrenaline, 5 mM dopamine, and 5 mM epinephrine at 530 nm in PB−DMSO (pH 5.0, 1:1, v/v) system, respectively. (d) Quantitative fluorescent intensities at 530 nm upon addition of 0, 50 μM, 100 μM, 200 μM, 500 μM, and 1 mM noradrenaline to 5 μM **FCS** containing detection system, respectively. The fluorescent intensity data were obtained 340 min after noradrenaline addition. Error bars represent standard deviations, n = 3; λ_{ex} = 510 nm, slit: 5 nm / 2.5 nm.

Noradrenaline Visualization in Brain Tissue. Supported by the spectroscopic data of **FCS** for noradrenaline detection, we wondered whether the probe could be used for noradrenergic neurons labeling in brain tissue. Noradrenergic neurons distribute in brainstem nucleus locus coeruleus. They can be distinguished over dopaminergic neurons via dual immunolabeling for DBH and TH which are essential enzymes for noradrenaline and its precursor dopamine synthesis, respectively. At the same time, adrenergic neurons can be visualized specifically by immunolabeling for PNMT which convert noradrenaline to epinephrine.[2,15,31] So we preformed dual immunofluorescence labeling experiments to visualize TH and DBH, or DBH and PNMT positive regions in coronal respectively which was then stained with **FCS** before imaging. As shown in Figure 4, the overall pattern of **FCS** (red, c) and DBH-AF350 (blue, b) fluorescent signals showed extensive overlap (pink, e) which demonstrated the excellent noradrenergic neurons specific labeling property of **FCS**. As a continuous work, Figure 5 displayed the discriminatory property of **FCS** toward noradrenaline over epinephrine. As shown in Figure 5d, **FCS** labeled noradrenergic neurons which were DBH positive could exactly be discriminated over adrenergic neurons (additional tissue images are shown in Figure S14-S17). These results mean that **FCS** represents an easier tool for noradrenergic neurons specific labeling over dopaminergic neurons and adrenergic neurons in brain tissue compared with the time consuming and complicated immunofluorescence labeling.

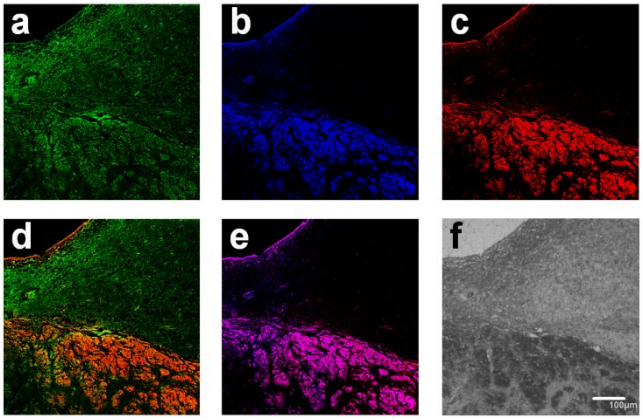

Figure 4. FCS labels noradrenergic neurons in brain tissue. a) Immunofluorescence Cy3 labeled TH positive region (green); b) Immunofluorescence AF350 labeled DBH positive region (blue); c) **FCS** labeled brain tissue (red); d) Merged image of a and c; e) Merged image of b and c; f) Bright field of the tissue. Cy3: λ_{ex} = 548 nm, λ_{em} = 560-610 nm; AF350: λ_{ex} = 405 nm, λ_{em} = 430-480 nm; **FCS**: λ_{ex} = 500 nm, λ_{em} = 510-560 nm; bar = 100 μm.

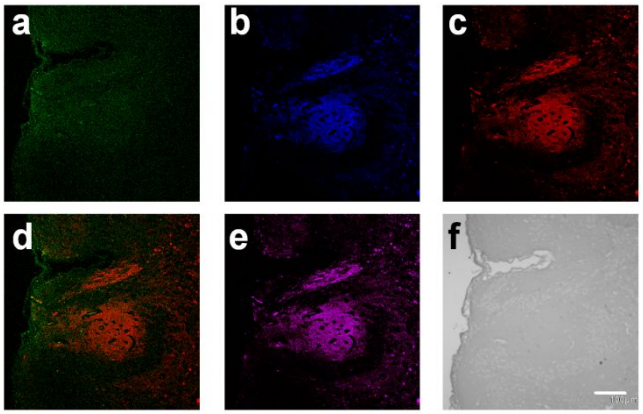

Figure 5. FCS labels noradrenergic neurons in brain tissue. a) Immunofluorescence Cy3 labeled PNMT positive region (green); b) Immunofluorescence AF350 labeled DBH positive region (blue); c) **FCS** labeled brain tissue (red); d) Merged image of a and c; e) Merged image of b and c; f) Bright field of the tissue. Cy3: λ_{ex} = 548 nm, λ_{em} = 560-610 nm; AF350: λ_{ex} = 405 nm, λ_{em} = 430-480 nm; **FCS**: λ_{ex} = 500 nm, λ_{em} = 510-560 nm; bar = 100 μm.

CONCLUSIONS

In conclusion, we utilized the cascade nucleophilic substitution reactions between noradrenaline and fluorophore coupling carbonic ester which formed a five-membered ring catechol-containing compound with the release of the fluorophore to develop a new generation of noradrenaline specific fluorescent probes design strategy. Promoted by the structural particularity of noradrenaline, the probes based on this strategy can effectively avoid the fluorescent quench caused by the catechol group through intramolecular PET process in NeuroSensor 521 with improved specificity. The accordingly synthesized probe **FCS** can detect and label noradrenaline both in aqueous solution and in brain tissue over dopamine and epinephrine. The present work provides an efficient tool for noradrenergic neurons visualization. To develop probes with fast and ratiometric fluorescent responses toward noradrenaline are on-going in our lab. We believe this

probe will promote the physiological and pathological studies of noradrenaline in brain.

AUTHOR INFORMATION

Corresponding Author

*E-mail: yincx@sxu.edu.cn. Tel./Fax: +86-351-7011022.

ORCID

Caixia Yin: 0000-0001-5548-6333

Notes

There are no conflicts to declare.

ACKNOWLEDGMENT

We thank the National Natural Science Foundation of China (No. 21672131, 21775096, 21705102), Talents Support Program of Shanxi Province (2014401), Shanxi Province Foundation for Returness (2017-026) and Scientific Instrument Center of Shanxi University.

ASSOCIATED CONTENT

Supporting Information

The Supporting Information is available free of charge on the ACS Publications website.

Synthesis of probes and the structure characterizations, additional fluorescence and UV-vis spectra, and additional fluorescence images (PDF)

REFERENCES

(1) Sara, S. J. The locus coeruleus and noradrenergic modulation of cognition. *Nat. Rev. Neurosci.* **2009**, *10*, 211-223.

(2) Rinaman, L. Hindbrain noradrenergic A2 neurons: diverse roles in autonomic, endocrine, cognitive, and behavioral functions. *Am. J. Physiol. Reg. I.* **2011**, *300*, R222-235.

(3) Armstrong, D. M.; Ross, C. A.; Pickel, V. M.; Joh, T. H.; Reis, D. J. Distribution of dopamine-, noradrenaline-, and adrenaline-containing cell bodies in the rat medulla oblongata: demonstrated by the immunocytochemical localization of catecholamine biosynthetic enzymes. *J. Comp. Neurol.* **1982**, *212*, 173-187.

(4) Lee, M.; Gubernator, N. G.; Sulzer, D.; Sames, D. Development of pH-responsive fluorescent false neurotransmitters. *J. Am. Chem. Soc.* **2010**, *132*, 8828-8830.

(5) Bundzikova-Osacka, J.; Ghosal, S.; Packard, B. A.; Ulrich-Lai, Y. M.; Herman, J. P. Role of nucleus of the solitary tract noradrenergic neurons in post-stress cardiovascular and hormonal control in male rats. *Stress* **2015**, *18*, 221-232.

(6) Dreyfus, N.; Myers, J. K.; Badescu, V. O.; de Frutos, O.; de la Puente, M. L.; Ding, C.; Filla, S. A.; Fynboe, K.; Gernert, D. L.; Heinz, B. A.; Hemrick-Luecke, S. K.; Johnson, K. W.; Johnson, M. P.; Lopez, P.; Love, P. L.; Martin, L. J.; Masquelin, T.; McCoy, M. J.; Mendiola, J.; Morrow, D.; Muhlhauser, M.; Pascual, G.; Perun, T. J.; Pfeifer, L. A.; Phebus, L. A.; Richards, S. J.; Rincon, J. A.; Seest, E. P.; Shah, J.; Shaojuan, J.; Simmons, R. M.; Stephenson, G. A.; Tromiczak, E. G.; Thompson, L. K.; Walter, M. W.; Weber, W. W.; Zarrinmayeh, H.; Thomas, C. E.; Joshi, E.; Iyengar, S.; Johansson, A. M. Discovery of a potent, dual serotonin and norepinephrine reuptake inhibitor. *ACS Med. Chem. Lett.* **2013**, *4*, 560-564.

(7) aan het Rot, M.; Mathew, S. J.; Charney, D. S. Neurobiological mechanisms in major depressive disorder. *Can. Med. Assoc. J.* **2009**, *180*, 305-313.

(8) Russell, J. A.; Walley, K. R.; Singer, J.; Gordon, A. C.; Hebert, P. C.; Cooper, D. J.; Holmes, C. L.; Mehta, S.; Granton, J. T.; Storms, M. M.; Cook, D. J.; Presneill, J. J.; Ayers, D.; Investigators, V. Vasopressin versus norepinephrine infusion in patients with septic shock. *The New Engl. J. Med.* **2008**, *358*, 877-887.

(9) De Backer , D.; Biston , P.; Devriendt , J.; Madl , C.; Chochrad , D.; Aldecoa , C.; Brasseur , A.; Defrance , P.; Gottignies , P.; Vincent , J. L. Comparison of dopamine and norepinephrine in the treatment of Shock. *New Engl. J. Med.* **2010**, *362*, 779-789.

(10) Pham, L.; Baker, M. R.; Shahanoor, Z.; Romeo, R. D. Adolescent changes in hindbrain noradrenergic A2 neurons in male rats. *Brain Res.* **2017**, *1666*, 11-16.

(11) Nakatsuka, N.; Andrews, A. M. Differentiating siblings: The case of dopamine and norepinephrine. *ACS Chem. Neurosci.* **2017**, *8*, 218-220.

(12) Cieslak, P. E.; Llamosas, N.; Kos, T.; Ugedo, L.; Jastrzebska, K.; Torrecilla, M.; Rodriguez Parkitna, J. The role of NMDA receptor-dependent activity of noradrenergic neurons in attention, impulsivity and exploratory behaviors. *Genes Brain Behav.* **2017**, *16*, 812-822.

(13) Bucci, D.; Busceti, C. L.; Calierno, M. T.; Di Pietro, P.; Madonna, M.; Biagioni, F.; Ryskalin, L.; Limanaqi, F.; Nicoletti, F.; Fornai, F. Systematic morphometry of catecholamine nuclei in the brainstem. *Front. Neuroanat.* **2017**, *11*, 98.

(14) Muller, A.; Joseph, V.; Slesinger, P. A.; Kleinfeld, D. Cell-based reporters reveal in vivo dynamics of dopamine and norepinephrine release in murine cortex. *Nat. Methods* **2014**, *11*, 1245-1252.

(15) Gubernator, N. G.; Zhang, H.; Staal, R. G.; Mosharov, E. V.; Pereira, D. B.; Yue, M.; Balsanek, V.; Vadola, P. A.; Mukherjee, B.; Edwards, R. H.; Sulzer, D.; Sames, D. Fluorescent false neurotransmitters visualize dopamine release from individual presynaptic terminals. *Science* **2009**, *324*, 1441-1444.

(16) Hu, G.; Henke, A.; Karpowicz, R. J., Jr.; Sonders, M. S.; Farrimond, F.; Edwards, R.; Sulzer, D.; Sames, D. New fluorescent substrate enables quantitative and high-throughput examination of vesicular monoamine transporter 2 (VMAT2). *ACS Chem. Biol.* **2013**, *8*, 1947-1954.

(17) Rodriguez, P. C.; Pereira, D. B.; Borgkvist, A.; Wong, M. Y.; Barnard, C.; Sonders, M. S.; Zhang, H.; Sames, D.; Sulzer, D. Fluorescent dopamine tracer resolves individual dopaminergic synapses and their activity in the brain. *P. Nati. Acad. Sci. USA* **2013**, *110*, 870-875.

(18) Pereira, D. B.; Schmitz, Y.; Meszaros, J.; Merchant, P.; Hu, G.; Li, S.; Henke, A.; Lizardi-Ortiz, J. E.; Karpowicz, R. J., Jr.; Morgenstern, T. J.; Sonders, M. S.; Kanter, E.; Rodriguez, P. C.; Mosharov, E. V.; Sames, D.; Sulzer, D. Fluorescent false neurotransmitter reveals functionally silent dopamine vesicle clusters in the striatum. *Nat. Neurosci.* **2016**, *19*, 578-586.

(19) Dunn, M.; Henke, A.; Clark, S.; Kovalyova, Y.; Kempadoo, K. A.; Karpowicz, R. J., Jr.; Kandel, E. R.; Sulzer, D.; Sames, D. Designing a norepinephrine optical tracer for imaging individual noradrenergic synapses and their activity in vivo. *Nat. Commun.* **2018**, *9*, 2838.

(20) Hettie, K. S.; Liu, X.; Gillis, K. D.; Glass, T. E. Selective catecholamine recognition with NeuroSensor 521: a fluorescent sensor for the visualization of norepinephrine in fixed and live cells. *ACS Chem. Neurosci.* **2013**, *4*, 918-923.

(21) Hettie, K. S.; Glass, T. E. Turn-on near-infrared fluorescent sensor for selectively imaging serotonin. *ACS Chem. Neurosci.* **2016**, *7*, 21-25.

(22) Hettie, K. S.; Glass, T. E. Coumarin-3-aldehyde as a scaffold for the design of tunable PET-modulated fluorescent sensors for neurotransmitters. *Chem. Eur. J.* **2014**, *20*, 17488-17499.

(23) Hettie, K. S.; Klockow, J. L.; Glass, T. E. Three-input logic gates with potential applications for neuronal imaging. *J. Am. Chem. Soc.* **2014**, *136*, 4877-4880.

(24) Feuster, E. K.; Glass, T. E. Detection of amines and unprotected amino acids in aqueous conditions by formation of highly fluorescent iminium ions. *J. Am. Chem. Soc.* **2003**, *125*, 16174-16175.

(25) Niu, L. Y.; Guan, Y. S.; Chen, Y. Z.; Wu, L. Z.; Tung, C. H.; Yang, Q. Z. BODIPY-based ratiometric fluorescent sensor for highly selective detection of glutathione over cysteine and homocysteine. *J. Am. Chem. Soc.* **2012**, *134*, 18928-18931.

(26) Liu, J.; Sun, Y. Q.; Huo, Y.; Zhang, H.; Wang, L.; Zhang, P.; Song, D.; Shi, Y.; Guo, W. Simultaneous fluorescence sensing of Cys

and GSH from different emission channels. *J. Am. Chem. Soc.* **2014**, *136*, 574-577.

(27) Yin, C. X.; Xiong, K. M.; Huo, F. J.; Salamanca, J. C.; Strongin, R. M. Fluorescent probes with multiple binding sites for the discrimination of Cys, Hcy, and GSH. *Angew. Chem. Int. Ed.* **2017**, *56*, 13188-13198.

(28) Yuan, L.; Lin, W.; Chen, H.; Zhu, S.; He, L. A unique family of rigid analogues of the GFP chromophore with tunable two-photon action cross-sections for biological imaging. *Angew. Chem. Int. Ed.* **2013**, *52*, 10018-10022.

(29) Laxman, S.; Sutter, B. M.; Wu, X.; Kumar, S.; Guo, X.; Trudgian, D. C.; Mirzaei, H.; Tu, B. P. Sulfur amino acids regulate translational capacity and metabolic homeostasis through modulation of tRNA thiolation. *Cell* **2013**, *154*, 416-429.

(30) Deshpande, A. A.; Bhatia, M.; Laxman, S.; Bachhawat, A. K. Thiol trapping and metabolic redistribution of sulfur metabolites enable cells to overcome cysteine overload. *Microbial Cell* **2017**, *4*, 112-126.

(31) Bathina, C. S.; Rajulapati, A.; Franzke, M.; Yamamoto, K.; Cunningham, J. T.; Mifflin, S. Knockdown of tyrosine hydroxylase in the nucleus of the solitary tract reduces elevated blood pressure during chronic intermittent hypoxia. *Am. J. Physiol. Reg. I.* **2013**, *305*, R1031-1039.

Insert Table of Contents artwork here